

## BLOCK-DIAGONALIZATION OF THE LINEARIZED COUPLED-MODE SYSTEM

MARINA CHUGUNOVA, DMITRY PELINOVSKY

**ABSTRACT.** We consider the Hamiltonian coupled-mode system that occur in nonlinear optics, photonics, and atomic physics. Spectral stability of gap solitons is determined by eigenvalues of the linearized coupled-mode system, which is equivalent to a four-by-four Dirac system with sign-indefinite metric. In the special class of symmetric nonlinear potentials, we construct a block-diagonal representation of the linearized equations, when the spectral problem reduces to two coupled two-by-two Dirac systems. The block-diagonalization is used in numerical computations of eigenvalues that determine stability of gap solitons.

### 1. INTRODUCTION

Various applications in nonlinear optics [1], photonics band-gap engineering [2] and atomic physics [3] call for systematic studies of the *coupled-mode system*, which is expressed by two first-order semi-linear PDEs in one space and one time dimensions. In nonlinear optics, the coupled-mode system describes counter-propagating light waves, which interact with a linear grating in an optical waveguide [4]. In photonics, the coupled-mode system is derived for coupled resonant waves in stop bands of a low-contrast three-dimensional photonic crystal [5]. In atomic physics, the coupled-mode system describes matter-wave Bose-Einstein condensates trapped in an optical lattice [6]. Existence, stability and nonlinear dynamics of *gap solitons*, which are localized solutions of the coupled-mode system, are fundamental problems for interest in the aforementioned physical disciplines.

In the context of spectral stability of gap solitons, it has been discovered that the linearized coupled-mode system is equivalent to a four-by-four Dirac system with sign-indefinite metric, where numerical computations of eigenvalues represent a difficult numerical task. The pioneer work in [7, 8] showed that spurious unstable eigenvalues originate from the continuous spectrum in the Fourier basis decomposition and the Galerkin approximation. A delicate but time-consuming implementation of the continuous Newton method was developed to identify true unstable eigenvalues from the spurious ones [7, 8]. Similar problems were discovered in the variational method [9, 10] and in the numerical finite-difference method [11, 12].

While some conclusions on instability bifurcations of gap solitons in the coupled-mode equations can be drawn on the basis of perturbation theory [7] and Evans function methods [13, 14], the numerical approximation of eigenvalues was an open

---

*Key words and phrases.* Hamiltonian coupled-mode systems, gap solitons, spectral stability, invariant subspaces, eigenvalues.

This work was completed with the support of the SharcNet Graduate Scholarship.

problem until recently. A new progress was made with the use of exterior algebra in the numerical computations of the Evans function [15], when the same results on instability bifurcations of gap solitons as in [7] were recovered. Similar shooting method was also applied to gap solitons in a more general model of a nonlinear Schrödinger equation with a periodic potential [6].

Our work addresses the problem of numerical approximations of eigenvalues of the linearized coupled-mode system with a different objective. We will show that the linearized coupled-mode system with a symmetric potential function can be block-diagonalized into two coupled two-by-two Dirac systems. The two Dirac systems represent the linearized Hamiltonian of the coupled-mode equations and determine instability bifurcations and unstable eigenvalues of gap solitons.

The purpose of block-diagonalization is twofold. First, the number of unstable eigenvalues and details of instability bifurcations can be investigated analytically from the number of non-zero isolated eigenvalues of the linearized Hamiltonian. This analysis will be reported in the forthcoming publication. Second, a numerical algorithm can be developed to compute efficiently the entire spectrum of the linearized coupled-mode system. These numerical results are reported here for an example of symmetric quadric potential functions.

The paper is organized as follows. Section 2 describes the model and its symmetries. Section 3 gives construction and properties of gap solitons in the nonlinear coupled-mode system. Section 4 presents block-diagonalization of the linearized coupled-mode system. Section 5 contains numerical computations of the spectrum of the block-diagonalized system. Appendix A presents derivation of exact solutions for gap solitons in the coupled-mode system with symmetric quadric potential functions.

## 2. COUPLED-MODE SYSTEM

We consider the Hamiltonian coupled-mode system in the form:

$$(2.1) \quad \begin{cases} i(u_t + u_x) + v = \partial_{\bar{u}} W(u, \bar{u}, v, \bar{v}) \\ i(v_t - v_x) + u = \partial_{\bar{v}} W(u, \bar{u}, v, \bar{v}) \end{cases}$$

where  $(u, v) \in \mathbb{C}^2$ ,  $x \in \mathbb{R}$ ,  $t \geq 0$ , and  $W(u, \bar{u}, v, \bar{v})$  is real-valued. We assume that the potential function satisfies the following three conditions:

- (1)  $W$  is invariant with respect to the gauge transformation:  $(u, v) \mapsto e^{i\alpha}(u, v)$ , for all  $\alpha \in \mathbb{R}$
- (2)  $W$  is symmetric with respect to the interchange:  $(u, v) \mapsto (v, u)$
- (3)  $W$  is analytic in its variables near  $u = v = 0$ , such that  $W = O(4)$ .

The first property is justified by the standard derivation of the coupled-mode system (2.1) with an envelope approximation [5]. The second property defines a class of symmetric nonlinear potentials. Although it is somewhat restrictive, symmetric nonlinear potentials are commonly met in physical applications of the system (2.1). The third property is related to the normal form analysis [16], where the nonlinear functions are approximated by Taylor polynomials. Since the quadratic part of the potential function is written in the left-hand-side of the system (2.1) and the cubic part violates the gauge transformation and analyticity assumptions, the Taylor polynomials of  $W$  start with quadric terms, denoted as  $O(4)$ .

We find a general representation of the function  $W(u, \bar{u}, v, \bar{v})$  that satisfies the conditions (1)-(3) and list all possible (four-parameter) quadric terms of  $W$ .

**Lemma 2.1.** *If  $W \in \mathbb{C}$  and property (1) is satisfied, such that*

$$(2.2) \quad W(u, \bar{u}, v, \bar{v}) = W(ue^{i\alpha}, \bar{u}e^{-i\alpha}, ve^{i\alpha}, \bar{v}e^{-i\alpha}), \quad \forall \alpha \in \mathbb{R},$$

*then  $W = W(|u|^2, |v|^2, u\bar{v})$ .*

*Proof.* By differentiating (2.2) in  $\alpha$  and setting  $\alpha = 0$ , we have the differential identity:

$$(2.3) \quad DW \equiv i \left( u \frac{\partial}{\partial u} - \bar{u} \frac{\partial}{\partial \bar{u}} + v \frac{\partial}{\partial v} - \bar{v} \frac{\partial}{\partial \bar{v}} \right) W(u, \bar{u}, v, \bar{v}) = 0.$$

Consider the set of quadratic variables

$$z_1 = |u|^2, \quad z_2 = |v|^2, \quad z_3 = \bar{u}v, \quad z_4 = u^2,$$

which is independent for any  $u \neq 0$  and  $v \neq 0$  in the sense that the Jacobian is non-zero. It is clear that  $Dz_{1,2,3} = 0$  and  $Dz_4 = 2z_4$ . Therefore,  $DW = 2z_4 \partial_{z_4} W = 0$ , such that  $W = W(z_1, z_2, z_3)$ .  $\square$

**Corollary 2.2.** *If  $W \in \mathbb{R}$  and property (1) is met, then  $W = W(|u|^2, |v|^2, u\bar{v} + v\bar{u})$ .*

**Lemma 2.3.** *If  $W \in \mathbb{R}$  and properties (1)-(3) are satisfied, then  $W = W(|u|^2 + |v|^2, |u|^2|v|^2, u\bar{v} + v\bar{u})$ .*

*Proof.* By Corollary 2.2 and property (2), we can re-order the arguments of  $W$  as  $W = W(|u| + |v|, |u||v|, u\bar{v} + v\bar{u})$ . By analyticity in property (3),  $W$  may depend only on  $|u|^2$  and  $|v|^2$  rather than on  $|u|$  and  $|v|$ .  $\square$

**Corollary 2.4.** *If  $W \in \mathbb{R}$  and properties (1)-(3) are satisfied, then*

$$(2.4) \quad \left( u \frac{\partial}{\partial u} + \bar{u} \frac{\partial}{\partial \bar{u}} - v \frac{\partial}{\partial v} - \bar{v} \frac{\partial}{\partial \bar{v}} \right) W(u, \bar{u}, v, \bar{v}) \Big|_{|u|^2=|v|^2} = 0$$

**Corollary 2.5.** *The only quadric potential function  $W \in \mathbb{R}$  that satisfies properties (1)-(3) is given by*

$$(2.5) \quad W = \frac{a_1}{2}(|u|^4 + |v|^4) + a_2|u|^2|v|^2 + a_3(|u|^2 + |v|^2)(v\bar{u} + \bar{v}u) + \frac{a_4}{2}(v\bar{u} + \bar{v}u)^2,$$

*where  $(a_1, a_2, a_3, a_4)$  are real-valued parameters. It follows then that*

$$\begin{cases} \frac{\partial W}{\partial u} = a_1|u|^2u + a_2u|v|^2 + a_3[(2|u|^2 + |v|^2)v + u^2\bar{v}] + a_4[v^2\bar{u} + |v|^2u] \\ \frac{\partial W}{\partial v} = a_1|v|^2v + a_2v|u|^2 + a_3[(2|v|^2 + |u|^2)u + v^2\bar{u}] + a_4[u^2\bar{v} + |u|^2v] \end{cases}$$

The potential function (2.5) with  $a_1, a_2 \neq 0$  and  $a_3 = a_4 = 0$  represents a standard coupled-mode system for a sub-harmonic resonance, e.g. in the context of optical gratings with constant Kerr nonlinearity [1]. When  $a_1 = a_3 = a_4 = 0$ , this system is integrable with inverse scattering and is referred to as the massive Thirring model [17]. When  $a_1 = a_2 = 0$  and  $a_3, a_4 \neq 0$ , the coupled-mode system corresponds to an optical grating with varying, mean-zero Kerr nonlinearity, where  $a_3$  is the Fourier coefficient of the resonant sub-harmonic and  $a_4$  is the Fourier coefficient of the non-resonant harmonic [5] (see also [4]).

We rewrite the coupled-mode system (2.1) as a Hamiltonian system in complex-valued matrix-vector notations:

$$(2.6) \quad \frac{d\mathbf{u}}{dt} = J\nabla H(\mathbf{u}),$$

where  $\mathbf{u} = (u, \bar{u}, v, \bar{v})^T$ ,

$$J = \begin{bmatrix} 0 & -i & 0 & 0 \\ i & 0 & 0 & 0 \\ 0 & 0 & 0 & -i \\ 0 & 0 & i & 0 \end{bmatrix} = -J^T,$$

and  $H(u, \bar{u}, v, \bar{v}) = \int_{\mathbb{R}} h(u, \bar{u}, v, \bar{v}) dx$  is the Hamiltonian functional with the density:

$$h = W(u, \bar{u}, v, \bar{v}) - (v\bar{u} + u\bar{v}) + \frac{i}{2}(u\bar{u}_x - u_x\bar{u}) - \frac{i}{2}(v\bar{v}_x - v_x\bar{v}).$$

The Hamiltonian  $H(u, \bar{u}, v, \bar{v})$  is constant in time  $t \geq 0$ . Due to the gauge invariance, the coupled-mode system (2.1) has another constant of motion  $Q(u, \bar{u}, v, \bar{v})$ , where

$$(2.7) \quad Q = \int_{\mathbb{R}} (|u|^2 + |v|^2) dx.$$

Conservation of  $Q$  can be checked by direct computation:

$$(2.8) \quad \frac{\partial}{\partial t}(|u|^2 + |v|^2) + \frac{\partial}{\partial x}(|u|^2 - |v|^2) = DW = 0,$$

where the operator  $D$  is defined in (2.3). Due to the translational invariance, the coupled-mode system (2.1) has yet another constant of motion  $P(u, \bar{u}, v, \bar{v})$ , where

$$(2.9) \quad P = \frac{i}{2} \int_{\mathbb{R}} (u\bar{u}_x - u_x\bar{u} + v\bar{v}_x - v_x\bar{v}) dx.$$

In applications, the quantities  $Q$  and  $P$  are referred to as the power and momentum of the coupled-mode system.

### 3. EXISTENCE OF GAP SOLITONS

*Stationary* solutions of the coupled-mode system (2.1) take the form:

$$(3.1) \quad \begin{cases} u_{\text{st}}(x, t) = u_0(x + s)e^{i\omega t + i\theta} \\ v_{\text{st}}(x, t) = v_0(x + s)e^{i\omega t + i\theta} \end{cases}$$

where  $(s, \theta) \in \mathbb{R}^2$  are arbitrary parameters, while the solution  $(u_0, v_0) \in \mathbb{C}^2$  on  $x \in \mathbb{R}$  and the domain for parameter  $\omega \in \mathbb{R}$  are to be found from the nonlinear ODE system:

$$(3.2) \quad \begin{cases} iu'_0 = \omega u_0 - v_0 + \partial_{\bar{u}_0} W(u_0, \bar{u}_0, v_0, \bar{v}_0) \\ -iv'_0 = \omega v_0 - u_0 + \partial_{\bar{v}_0} W(u_0, \bar{u}_0, v_0, \bar{v}_0) \end{cases}$$

Stationary solutions are critical points of the Lyapunov functional:

$$(3.3) \quad \Lambda = H(u, \bar{u}, v, \bar{v}) + \omega Q(u, \bar{u}, v, \bar{v}),$$

such that variations of  $\Lambda$  produce the nonlinear ODE system (3.2).

**Lemma 3.1.** *Assume that there exists a decaying solution  $(u_0, v_0)$  of the system (3.2) on  $x \in \mathbb{R}$ . If  $W \in \mathbb{R}$  satisfies properties (1)-(3), then  $u_0 = \bar{v}_0$  (module to an arbitrary phase).*

*Proof.* It follows from the balance equation (2.8) for the stationary solutions (3.1) that

$$|u_0|^2 - |v_0|^2 = C_0 = 0, \quad \forall x \in \mathbb{R},$$

where the constant  $C_0 = 0$  is found from decaying conditions at infinity. Let us represent the solutions  $(u_0, v_0)$  in the form:

$$(3.4) \quad \begin{cases} u_0(x) = \sqrt{Q(x)} e^{i\Theta(x) + i\Phi(x)} \\ v_0(x) = \sqrt{Q(x)} e^{-i\Theta(x) + i\Phi(x)} \end{cases}$$

such that

$$(3.5) \quad \begin{cases} iQ' - 2Q(\Theta' + \Phi') = 2\omega Q - 2Qe^{-2i\Theta} + 2\bar{u}_0 \partial_{\bar{u}_0} W(u_0, \bar{u}_0, v_0, \bar{v}_0) \\ -iQ' - 2Q(\Theta' - \Phi') = 2\omega Q - 2Qe^{2i\Theta} + 2\bar{v}_0 \partial_{\bar{v}_0} W(u_0, \bar{u}_0, v_0, \bar{v}_0) \end{cases}$$

Separating the real parts, we obtain

$$(3.6) \quad \begin{cases} Q(\cos(2\Theta) - \omega - \Theta' - \Phi') = \text{Re} [\bar{u}_0 \partial_{\bar{u}_0} W(u_0, \bar{u}_0, v_0, \bar{v}_0)] \\ Q(\cos(2\Theta) - \omega - \Theta' + \Phi') = \text{Re} [\bar{v}_0 \partial_{\bar{v}_0} W(u_0, \bar{u}_0, v_0, \bar{v}_0)] \end{cases}$$

By Corollary 2.4, we have  $\Phi' \equiv 0$ , such that  $\Phi(x) = \Phi_0$ .  $\square$

**Corollary 3.2.** *Let  $u_0 = \bar{v}_0$ . The ODE system (3.2) reduces to the planar Hamiltonian form:*

$$(3.7) \quad \frac{d}{dx} \begin{pmatrix} p \\ q \end{pmatrix} = \begin{pmatrix} 0 & -1 \\ +1 & 0 \end{pmatrix} \nabla h(p, q),$$

where  $p = 2\Theta$ ,  $q = Q$ , and

$$(3.8) \quad h = \tilde{W}(p, q) - 2q \cos p + 2\omega q, \quad \tilde{W}(p, q) = W(u_0, \bar{u}_0, v_0, \bar{v}_0).$$

*Proof.* In variables  $(Q, \Theta)$  defined by (3.4) with  $\Phi(x) = \Phi_0 = 0$ , we rewrite the ODE system (3.5) as follows:

$$(3.9) \quad \begin{cases} Q' = 2Q \sin(2\Theta) + 2\text{Im} [\bar{u}_0 \partial_{\bar{u}_0} W(u_0, \bar{u}_0, v_0, \bar{v}_0)] \\ Q\Theta' = -\omega Q + Q \cos(2\Theta) - \text{Re} [\bar{u}_0 \partial_{\bar{u}_0} W(u_0, \bar{u}_0, v_0, \bar{v}_0)] \end{cases}$$

The system (3.9) is equivalent to the Hamiltonian system (3.7) and (3.8) if

$$(3.10) \quad \begin{cases} \partial_p \tilde{W}(p, q) = i [u_0 \partial_{u_0} - \bar{u}_0 \partial_{\bar{u}_0}] W(u_0, \bar{u}_0, v_0, \bar{v}_0) \\ q \partial_q \tilde{W}(p, q) = [u_0 \partial_{u_0} + \bar{u}_0 \partial_{\bar{u}_0}] W(u_0, \bar{u}_0, v_0, \bar{v}_0) \end{cases}$$

The latter equations follows from (2.3), (2.4), and (3.4) with the chain rule.  $\square$

**Corollary 3.3.** *Let  $u_0 = \bar{v}_0$ . Then,*

$$(3.11) \quad \partial_{u_0 \bar{u}_0}^2 W = \partial_{v_0 \bar{v}_0}^2 W, \quad \partial_{\bar{u}_0^2}^2 W = \partial_{v_0^2}^2 W, \quad \partial_{u_0 v_0}^2 W = \partial_{\bar{u}_0 \bar{v}_0}^2 W.$$

*Remark 3.4.* The family of stationary solutions (3.1) can be extended to the family of travelling solutions of the coupled-mode system (2.1) by means of the Lorentz transformation [15]. With the boosted variables,

$$X = \frac{x - ct}{\sqrt{1 - c^2}}, \quad T = \frac{t - cx}{\sqrt{1 - c^2}}, \quad U = \left( \frac{1 - c}{1 + c} \right)^{1/4} u, \quad V = \left( \frac{1 + c}{1 - c} \right)^{1/4} v,$$

where  $c \in (-1, 1)$ , the family of travelling solutions still satisfies the constraint  $|U_0|^2 = |V_0|^2$  from the balance equation (2.8). However, Corollary 2.4 fails for a boosted potential function  $\tilde{W}(U, \bar{U}, V, \bar{V})$  and the representation (3.4) results no longer in the relation  $U_0 = \bar{V}_0$  [7]. It will be studied separately if the block-diagonalization of the linearized coupled-mode system can be extended (in a non-trivial matter) to the family of travelling solutions.

Decaying solutions of the system (3.2) with a homogeneous polynomial function  $W(u, \bar{u}, v, \bar{v})$  are analyzed in Appendix A. Conditions for their existence are identified for the quadratic potential function (2.5). Decaying solutions may exist in the gap of continuous spectrum of the coupled-mode system (2.1) for  $\omega \in (-1, 1)$ . We introduce two auxiliary parameters:

$$(3.12) \quad \mu = \frac{1 - \omega}{1 + \omega}, \quad \beta = \sqrt{1 - \omega^2},$$

such that  $0 < \mu < \infty$  and  $0 < \beta \leq 1$ . When  $a_1 = 1$ ,  $a_2 = \rho$ , and  $a_3 = a_4 = 0$ , we obtain in Appendix A the decaying solution  $u_0(x)$  in the explicit form:

$$(3.13) \quad u_0 = \sqrt{\frac{2(1 - \omega)}{1 + \rho}} \frac{1}{(\cosh \beta x + i\sqrt{\mu} \sinh \beta x)}.$$

When  $\omega \rightarrow 1$  (such that  $\mu \rightarrow 0$  and  $\beta \rightarrow 0$ ), the decaying solution (3.13) becomes small in absolute value and approaches the limit of sech-solutions  $\text{sech}(\beta x)$ . When  $\omega \rightarrow -1$  (such that  $\mu \rightarrow \infty$  and  $\beta \rightarrow 0$ ), the decaying solution (3.13) remains finite in absolute value and approaches the limit of the algebraically decaying solution:

$$u_0 = \frac{2}{\sqrt{1 + \rho}(1 + 2ix)}.$$

When  $a_1 = a_2 = 0$ ,  $a_3 = 1$  and  $a_4 = s$ , the decaying solution  $u_0(x)$  exists in two sub-domains:  $\omega > 0$ ,  $s > -1$  and  $\omega < 0$ ,  $s < 1$ . When  $\omega > 0$ ,  $s > -1$ , the solution takes the form:

$$(3.14) \quad u_0 = \sqrt{\frac{1 - \omega}{2}} \frac{(\cosh \beta x - i\sqrt{\mu} \sinh \beta x)}{\sqrt{\Delta_+(x)}},$$

where

$$\Delta_+ = [(s - 1)\mu^2 - 2s\mu + (s + 1)] \cosh^4(\beta x) + 2[s\mu - (s - 1)\mu^2] \cosh^2(\beta x) + (s - 1)\mu^2.$$

When  $\omega < 0$ ,  $s < 1$ , the solution takes the form:

$$(3.15) \quad u_0 = \sqrt{\frac{1 - \omega}{2}} \frac{(\sinh \beta x - i\sqrt{\mu} \cosh \beta x)}{\sqrt{\Delta_-(x)}}.$$

where

$$\Delta_- = [(s + 1) - 2s\mu - (s - 1)\mu^2] \cosh^4(\beta x) + 2[s + 1 - s\mu] \cosh^2(\beta x) - (s + 1).$$

In both limits  $\omega \rightarrow 1$  and  $\omega \rightarrow -1$ , the decaying solutions (3.14) and (3.15) approach the small-amplitude sech-solution  $\text{sech}(\beta x)$ . In the limit  $\omega \rightarrow 0$ , the decaying solutions (3.14) and (3.15) degenerate into a non-decaying bounded solution with  $|u_0(x)|^2 = \frac{1}{2}$ .

#### 4. BLOCK-DIAGONALIZATION OF THE LINEARIZED SYSTEM

Linearization of the coupled-mode system (2.1) at the stationary solutions (3.1) with  $s = \theta = 0$  is defined as follows:

$$(4.1) \quad \begin{cases} u(x, t) = e^{i\omega t} (u_0(x) + U_1(x)e^{\lambda t}) \\ \bar{u}(x, t) = e^{-i\omega t} (\bar{u}_0(x) + U_2(x)e^{\lambda t}) \\ v(x, t) = e^{i\omega t} (v_0(x) + U_3(x)e^{\lambda t}) \\ \bar{v}(x, t) = e^{-i\omega t} (\bar{v}_0(x) + U_4(x)e^{\lambda t}) \end{cases}$$

where  $v_0 = \bar{u}_0$ , according to Lemma 3.1. Let  $(\mathbf{f}, \mathbf{g})$  be a standard inner product for  $\mathbf{f}, \mathbf{g} \in L^2(\mathbb{R}, \mathbb{C}^4)$ . Expanding the Lyapunov functional (3.3) into Taylor series near  $\mathbf{u}_0 = (u_0, \bar{u}_0, v_0, \bar{v}_0)^T$ , we have:

$$(4.2) \quad \Lambda = \Lambda(\mathbf{u}_0) + (\mathbf{U}, \nabla \Lambda|_{\mathbf{u}_0}) + \frac{1}{2}(\mathbf{U}, H_\omega \mathbf{U}) + \dots,$$

where  $\mathbf{U} = (U_1, U_2, U_3, U_4)^T$  and  $H_\omega$  is the the linearized energy operator in the explicit form

$$(4.3) \quad H_\omega = D(\partial_x) + V(x),$$

where

$$(4.4) \quad D = \begin{pmatrix} \omega - i\partial_x & 0 & -1 & 0 \\ 0 & \omega + i\partial_x & 0 & -1 \\ -1 & 0 & \omega + i\partial_x & 0 \\ 0 & -1 & 0 & \omega - i\partial_x \end{pmatrix}$$

and

$$(4.5) \quad V = \begin{pmatrix} \partial_{\bar{u}_0 u_0}^2 & \partial_{\bar{u}_0^2}^2 & \partial_{\bar{u}_0 v_0}^2 & \partial_{\bar{u}_0 \bar{v}_0}^2 \\ \partial_{u_0^2}^2 & \partial_{u_0 \bar{u}_0}^2 & \partial_{u_0 v_0}^2 & \partial_{u_0 \bar{v}_0}^2 \\ \partial_{\bar{v}_0 u_0}^2 & \partial_{\bar{v}_0 \bar{u}_0}^2 & \partial_{\bar{v}_0 v_0}^2 & \partial_{\bar{v}_0^2}^2 \\ \partial_{v_0 u_0}^2 & \partial_{v_0 \bar{u}_0}^2 & \partial_{v_0^2}^2 & \partial_{v_0 \bar{v}_0}^2 \end{pmatrix} W(u_0, \bar{u}_0, v_0, \bar{v}_0).$$

The linearization (4.1) of the nonlinear coupled-mode system (2.1) results in the linearized coupled-mode system in the form:

$$(4.6) \quad H_\omega \mathbf{U} = i\lambda \sigma \mathbf{U},$$

where  $\sigma$  is a diagonal matrix of  $(1, -1, 1, -1)$ . Due to the gauge and translational symmetries, the energy operator  $H_\omega$  has a non-empty kernel which includes two eigenvectors:

$$(4.7) \quad \mathbf{U}_1 = \sigma \mathbf{u}_0(x), \quad \mathbf{U}_2 = \mathbf{u}'_0(x).$$

The eigenvectors  $\mathbf{U}_{1,2}$  represent derivatives of the stationary solutions (3.1) with respect to parameters  $(\theta, s)$ . We adopt a standard assumption that the coupled-mode system is generic.

**Assumption 4.1.** *The kernel of  $H_\omega$  is exactly two-dimensional with the eigenvectors (4.7).*

Due to the Hamiltonian structure, the linearized operator  $\sigma H_\omega$  has at least four-dimensional generalized kernel with the eigenvectors (4.7) and two generalized eigenvectors (see [18] for details). The eigenvectors of the linearized operator  $\sigma H_\omega$  satisfy the  $\sigma$ -orthogonality constraints:

$$(4.8) \quad (\mathbf{u}_0, \mathbf{U}) = \int_{\mathbb{R}} (\bar{u}_0 U_1 + u_0 U_2 + \bar{v}_0 U_3 + v_0 U_4) dx = 0,$$

$$(4.9) \quad (\mathbf{u}'_0, \sigma \mathbf{U}) = \int_{\mathbb{R}} (\bar{u}'_0 U_1 - u'_0 U_2 + \bar{v}'_0 U_3 - v'_0 U_4) dx = 0.$$

The constraints (4.8) and (4.9) represent first variations of the conserved quantities  $Q$  and  $P$  in (2.7) and (2.9) at the linearization (4.1).

It follows from the explicit form of  $H_\omega$  and from Corollary 3.3 that the eigenvalue problem  $H_\omega \mathbf{U} = \mu \mathbf{U}$  has two reductions:

$$(4.10) \quad (i) U_1 = U_4, U_2 = U_3, \quad (ii) U_1 = -U_4, U_2 = -U_3.$$

Our main result on the block-diagonalization of the energy operator  $H_\omega$  and the linearized coupled-mode system (4.6) is based on the reductions (4.10).

**Theorem 4.2.** *Let  $W \in \mathbb{R}$  satisfy properties (1)-(3). Let  $(u_0, v_0)$  be a decaying solution of the system (3.2) on  $x \in \mathbb{R}$ , where  $v_0 = \bar{u}_0$ . There exists an orthogonal similarity transformation  $S$ , such that  $S^{-1} = S^T$ , where*

$$S = \frac{1}{\sqrt{2}} \begin{pmatrix} 1 & 0 & 1 & 0 \\ 0 & 1 & 0 & 1 \\ 0 & 1 & 0 & -1 \\ 1 & 0 & -1 & 0 \end{pmatrix},$$

that simultaneously block-diagonalizes the energy operator  $H_\omega$ ,

$$(4.11) \quad S^{-1} H_\omega S = \begin{pmatrix} H_+ & 0 \\ 0 & H_- \end{pmatrix} \equiv H,$$

and the linearized operator  $\sigma H_\omega$

$$(4.12) \quad S^{-1} \sigma H_\omega S = \sigma \begin{pmatrix} 0 & H_- \\ H_+ & 0 \end{pmatrix} \equiv iL,$$

where  $H_\pm$  are two-by-two Dirac operators:

$$(4.13) \quad H_\pm = \begin{pmatrix} \omega - i\partial_x & \mp 1 \\ \mp 1 & \omega + i\partial_x \end{pmatrix} + V_\pm(x),$$

and

$$(4.14) \quad V_\pm = \begin{pmatrix} \partial_{u_0 u_0}^2 \pm \partial_{u_0 v_0}^2 & \partial_{\bar{u}_0}^2 \pm \partial_{u_0 v_0}^2 \\ \partial_{u_0}^2 \pm \partial_{u_0 v_0}^2 & \partial_{\bar{u}_0 u_0}^2 \pm \partial_{u_0 v_0}^2 \end{pmatrix} W(u_0, \bar{u}_0, v_0, \bar{v}_0).$$

*Proof.* Applying the similarity transformation to the operator  $D(\partial_x)$  in (4.4), we have the first terms in Dirac operators  $H_\pm$ . Applying the same transformation to the potential  $V(x)$  in (4.5) and using Corollary 3.3, we have the second term in the Dirac operators  $H_\pm$ . The same transformation is applied similarly to the linearized operator  $\sigma H_\omega$  with the result (4.12).  $\square$

**Corollary 4.3.** *The linearized coupled-mode system (4.6) is equivalent to the block-diagonalized eigenvalue problems*

$$(4.15) \quad \sigma_3 H_- \sigma_3 H_+ \mathbf{V}_1 = \gamma \mathbf{V}_1, \quad \sigma_3 H_+ \sigma_3 H_- \mathbf{V}_2 = \gamma \mathbf{V}_2, \quad \gamma = -\lambda^2,$$

where  $\mathbf{V}_{1,2} \in \mathbb{C}^2$  and  $\sigma_3$  is the Pauli's diagonal matrix of  $(1, -1)$ .

**Corollary 4.4.** *Let  $\mathbf{u}_0 = (u_0, \bar{u}_0) \in \mathbb{C}^2$  and  $(\mathbf{f}, \mathbf{g})$  be a standard inner product for  $\mathbf{f}, \mathbf{g} \in L^2(\mathbb{R}, \mathbb{C}^2)$ . Dirac operators  $H_\pm$  have simple kernels with the eigenvectors*

$$(4.16) \quad H_+ \mathbf{u}'_0 = 0, \quad H_- \sigma_3 \mathbf{u}_0 = 0,$$

while the vectors  $\mathbf{V}_{1,2}$  satisfy the constraints

$$(4.17) \quad (\mathbf{u}_0, \mathbf{V}_1) = 0, \quad (\mathbf{u}'_0, \sigma_3 \mathbf{V}_2) = 0.$$

*Remark 4.5.* Block-diagonalization described in Theorem 4.2 has nothing in common with the explicit diagonalization used in reduction (9.2) of [14] for the particular potential function (2.5) with  $a_1 = a_2 = a_4 = 0$  and  $a_3 = 1$ . Moreover, the reduction (9.2) of [14] does not work for  $\omega \neq 0$ , while gap solitons do not exist in this particular model for  $\omega = 0$ .

We illustrate block-diagonalization of the eigenvalue problem (4.15) for the quadric potential function (2.5). When  $a_1 = 1$ ,  $a_2 = \rho$  and  $a_3 = a_4 = 0$ , the decaying solution  $u_0(x)$  is given by (3.13) and the potential matrices  $V_{\pm}(x)$  in the Dirac operators  $H_{\pm}$  in (4.13)–(4.14) are found in the explicit form:

$$(4.18) \quad V_+ = (1 + \rho) \begin{pmatrix} 2|u_0|^2 & u_0^2 \\ \bar{u}_0^2 & 2|u_0|^2 \end{pmatrix}, \quad V_- = \begin{pmatrix} 2|u_0|^2 & (1 - \rho)u_0^2 \\ (1 - \rho)\bar{u}_0^2 & 2|u_0|^2 \end{pmatrix}.$$

When  $a_1 = a_2 = 0$ ,  $a_3 = 1$  and  $a_4 = s$ , the decaying solution  $u_0(x)$  is given by either (3.14) or (3.15) and the potential matrices  $V_{\pm}(x)$  take the form:

$$(4.19) \quad V_+ = 3 \begin{pmatrix} u_0^2 + \bar{u}_0^2 & 2|u_0|^2 \\ 2|u_0|^2 & u_0^2 + \bar{u}_0^2 \end{pmatrix} + s \begin{pmatrix} 2|u_0|^2 & u_0^2 + 3\bar{u}_0^2 \\ \bar{u}_0^2 + 3u_0^2 & 2|u_0|^2 \end{pmatrix},$$

$$(4.20) \quad V_- = \begin{pmatrix} u_0^2 + \bar{u}_0^2 & -2|u_0|^2 \\ -2|u_0|^2 & u_0^2 + \bar{u}_0^2 \end{pmatrix} + s \begin{pmatrix} 0 & -u_0^2 - \bar{u}_0^2 \\ -u_0^2 - \bar{u}_0^2 & 0 \end{pmatrix}.$$

Numerical computations of eigenvalues of the Dirac operators  $H_{\pm}$  and the linearized operator  $L$  in (4.11) and (4.12) are developed for the explicit examples (4.18) and (4.19)–(4.20).

## 5. NUMERICAL COMPUTATIONS OF EIGENVALUES

Numerical discretization and truncation of the linearized coupled-mode system (4.6) leads to an eigenvalue problem for large matrices [19]. Parallel software libraries were recently developed for computations of large eigenvalue problems [20]. We shall use Scalapack library and distribute computations of eigenvalues of the system (4.6) for different parameter values between parallel processors of the SHARCnet cluster Idra using Message Passing Interface [21].

We implement a numerical discretization of the linearized coupled-mode system (4.6) using the Chebyshev interpolation method [22]. The main advantage of the Chebyshev grid is that clustering of the grid points occurs near the end points of the interval and this clustering prevents the appearance of spurious complex eigenvalues from the discretization of the continuous spectrum. If the eigenvector is analytic in a strip near the interpolation interval, the corresponding Chebyshev spectral derivatives converge geometrically, with an asymptotic convergence factor determined by the size of the largest ellipse in the domain of analyticity [22].

The continuous spectrum for the linearized coupled-mode system (4.6) can be found from the no-potential case  $V(x) \equiv 0$ . It consists of two pairs of symmetric branches on the imaginary axis  $\lambda \in i\mathbb{R}$  for  $|\text{Im}(\lambda)| > 1 - \omega$  and  $|\text{Im}(\lambda)| > 1 + \omega$  [7, 15]. In the potential case  $V(x) \neq 0$ , the continuous spectrum does not move, but the discrete spectrum appears. The discrete spectrum is represented by symmetric pairs or quartets of isolated non-zero eigenvalues and zero eigenvalue of algebraic multiplicity four for the generalized kernel of  $\sigma H_{\omega}$  [7, 15]. We note that symmetries of the Chebyshev grid preserve symmetries of the linearized coupled-mode system (4.6).

We shall study eigenvalues of the energy operator  $H_\omega$ , in connection to eigenvalues of the linearized operator  $\sigma H_\omega$ . It is well known [19, 22] that Hermitian matrices have condition number one, while non-Hermitian matrices may have large condition number. As a result, numerical computations for eigenvalues and eigenvectors have better accuracy and faster convergence for self-adjoint operators [19, 22]. We will use the block-diagonalizations (4.11) and (4.12) and compute eigenvalues of  $H_+$ ,  $H_-$ , and  $L$ . The block-diagonalized matrix can be stored in a special format which requires twice less memory than a full matrix and it accelerates computations of eigenvalues approximately in two times.

Figure 1 displays the pattern of eigenvalues and instability bifurcations for the symmetric quadric potential (2.5) with  $a_1 = 1$  and  $a_2 = a_3 = a_4 = 0$ . The decaying solution  $u_0(x)$  and the potential matrices  $V_\pm(x)$  are given by (3.13) and (4.18) with  $\rho = 0$ . Parameter  $\omega$  of the decaying solution  $u_0(x)$  is defined in the interval  $-1 < \omega < 1$ . Six pictures of Fig. 1 shows the entire spectrum of  $L$ ,  $H_+$  and  $H_-$  for different values of  $\omega$ . (The continuous movie that shows transformation of eigenvalues when  $\omega$  decreases is available as a multi-media attachment to this article.)

When  $\omega$  is close to 1 (the gap soliton is close to a small-amplitude sech-soliton), there exists a single non-zero eigenvalue for  $H_+$  and  $H_-$  and a single pair of purely imaginary eigenvalues of  $L$  (see subplot (1) on Fig. 1). The first set of arrays on the subplot (1) indicates that the pair of eigenvalues of  $L$  becomes visible at the same value of  $\omega$  as the eigenvalue of  $H_+$ . This correlation between eigenvalues of  $L$  and  $H_+$  can be traced throughout the entire parameter domain on the subplots (1)–(6).

When  $\omega$  decreases, the operator  $H_-$  acquires another non-zero eigenvalue by means of the edge bifurcation [13], with no changes in the number of isolated eigenvalues of  $L$  (see subplot (2)). The first complex instability occurs near  $\omega \approx -0.18$ , when the pair of purely imaginary eigenvalues of  $L$  collides with the continuous spectrum and emerge as a quartet of complex eigenvalues, with no changes in the number of isolated eigenvalues for  $H_+$  and  $H_-$  (see subplot (3)).

The second complex instability occurs at  $\omega \approx -0.54$ , when the operator  $H_-$  acquires a third non-zero eigenvalue and the linearized operator  $L$  acquires another quartet of complex eigenvalues (see subplot (4)). The second set of arrays on the subplots (4)–(6) indicates a correlation between these eigenvalues of  $L$  and  $H_-$ .

When  $\omega$  decreases further, the operators  $H_+$  and  $H_-$  acquires one more isolated eigenvalue, with no change in the spectrum of  $L$  (see subplot (5)). Finally, when  $\omega$  is close to  $-1$  (the gap soliton is close to the large-amplitude algebraic soliton), the third complex instability occurs, correlated with another edge bifurcation in the operator  $H_-$  (see subplot (6)). The third set of arrays on subplot (6) indicates this correlation. The third complex instability was missed in the previous numerical studies of the same system [7, 15]. In a narrow domain near  $\omega = -1$ , the operator  $H_+$  has two non-zero eigenvalues, the operator  $H_-$  has five non-zero eigenvalues and the operator  $L$  has three quartets of complex eigenvalues.

Figure 2 displays the pattern of eigenvalues and instability bifurcations for the symmetric quadric potential (2.5) with  $a_1 = a_2 = a_4 = 0$  and  $a_3 = 1$ . The decaying solution  $u_0(x)$  and the potential matrices  $V_\pm(x)$  are given by (3.14) and (4.19) with  $\omega > 0$  and  $s = 0$ . Eigenvalues in the other case  $\omega < 0$  can be found from those in the case  $\omega > 0$  by reflections.

When  $\omega$  is close to 1 (the gap soliton is close to a small-amplitude sech-soliton), there exists one non-zero eigenvalue of  $H_-$  and no non-zero eigenvalues of  $L$  and  $H_+$  (see subplot (1)). When  $\omega$  decreases, two more non-zero eigenvalues bifurcate in  $H_-$  from the left and right branches of the continuous spectrum, with no change in non-zero eigenvalues of  $L$  (see subplot (2)). The first complex bifurcation occurs at  $\omega \approx 0.45$ , when a quartet of complex eigenvalues occurs in  $L$ , in correlation with two symmetric edge bifurcations of  $H_+$  from the left and right branches of the continuous spectrum (see subplot (3)). The first and only set of arrays on the subplots (3)-(6) indicates a correlation between eigenvalues of  $L$  and  $H_+$ , which is traced through the remaining parameter domain of  $\omega$ . The inverse complex bifurcation occurs at  $\omega \approx 0.15$ , when the quartet of complex eigenvalues merge at the edge of the continuous spectrum into a pair of purely imaginary eigenvalues (see subplot (5)). No new eigenvalue emerge for smaller values of  $\omega$ . When  $\omega$  is close to 0 (the gap soliton is close to the non-decaying solution), the operator  $H_+$  has two non-zero eigenvalues, the operator  $H_-$  has three non-zero eigenvalues and the operator  $L$  has one pair of purely imaginary eigenvalues (see subplot (6)).

We mention two other limiting cases of the symmetric quadric potential (2.5). When  $a_1 = a_3 = a_4 = 0$  and  $a_2 = 1$ , the coupled-mode system is an integrable model and no non-zero eigenvalues of  $L$  exist, according to the exact solution of the linearization problem [9, 10]. When  $a_1 = a_2 = a_3 = 0$  and  $a_4 = \pm 1$ , one branch of decaying solutions  $u_0(x)$  exists for either sign, according to (3.14) and (3.15). The pattern of eigenvalues and instability bifurcations repeats that of Fig. 2.

Numerical results reported above imply that the number of isolated non-zero eigenvalues of the linearized operator  $L$  is bounded from above by the total number of non-zero isolated eigenvalues of the energy operators  $H_+$  and  $H_-$ . Furthermore, there exists a correlation between edge bifurcations in the operator  $L$  and those in the Dirac operators  $H_+$  and  $H_-$ . These analytical questions will be addressed in the future work.

#### APPENDIX A. CONDITIONS FOR EXISTENCE OF GAP SOLITONS IN THE HOMOGENEOUS POTENTIAL FUNCTION

We shall consider the homogeneous potential function  $W \in \mathbb{R}$  of the monomial order  $2n$  that satisfies properties (1)-(3). The general representation of  $W(u, \bar{u}, v, \bar{v})$  is given by

$$(A.1) \quad W = \sum_{s=0}^n \sum_{k=0}^{n-s} a_{k,s} (u^s \bar{v}^s + \bar{u}^s v^s) |u|^{2n-2k-2s} |v|^{2k},$$

where  $a_{k,s}$  are real-valued coefficients which are subject to the symmetry conditions:  $a_{k_1,s} = a_{k_2,s}$  if  $k_1 + k_2 = n - s$  for  $s = 0, 1, \dots, n-1$ . Let's introduce new parameters

$$A_s = \sum_{k=0}^{n-s} a_{k,s}, \quad s = 0, 1, \dots, n.$$

Using the variables  $(Q, \Theta)$  defined in (3.4) with  $\Phi(x) = \Phi_0 = 0$ , we rewrite the ODE system (3.7) in the explicit form:

$$(A.2) \quad \begin{cases} Q' = 2Q \sin(2\Theta) - 2Q^n \sum_{s=0}^n s A_s \sin(2s\Theta) \\ \Theta' = -\omega + \cos(2\Theta) - nQ^{n-1} \sum_{s=0}^n A_s \cos(2s\Theta) \end{cases}$$

There exists a first integral of the system (A.2):

$$-\omega Q + \cos(2\Theta)Q - Q^n \sum_{s=0}^n A_s \cos(2s\Theta) = C_0,$$

where  $C_0 = 0$  from the zero boundary conditions  $Q(x) \rightarrow 0$  as  $|x| \rightarrow \infty$ . As a result, the second-order system (A.2) is reduced to the first-order ODE

$$(A.3) \quad \Theta'(x) = (n-1)(\omega - \cos(2\Theta)),$$

while the function  $Q(x) \geq 0$  can be found from  $\Theta(x)$  as follows:

$$(A.4) \quad Q^{n-1} = \frac{(\cos(2\Theta) - \omega)}{\sum_{s=0}^n A_s \cos(2s\Theta)}.$$

We consider the quadric potential function  $W$  given by (2.5). Using (A.3) for the case  $n = 2$  we obtain:

$$(A.5) \quad \Theta'(x) = \omega - \cos(2\Theta),$$

and the correspondence:

$$A_0 = \frac{a_1 + a_2 + a_4}{2}, \quad A_1 = 2a_3, \quad A_2 = \frac{a_4}{2}.$$

We rewrite the representation (A.4) for  $Q(x)$  as follows:

$$(A.6) \quad Q = \frac{(t - \omega)}{\phi(t)}; \quad Q \geq 0$$

where

$$t = \cos(2\Theta), \quad \phi(t) = a_4 t^2 + 2a_3 t + \frac{a_1 + a_2}{2},$$

such that  $t \in [-1, 1]$ . Let's consider two cases:

$$(A.7) \quad \begin{cases} t \geq \omega; & \phi(t) \geq 0 & \Rightarrow Q^+ \\ t \leq \omega; & \phi(t) \leq 0 & \Rightarrow Q^- \end{cases}$$

We can solve the first-order ODE (A.5) using the substitution  $z = \tan(\Theta)$ , such that

$$t = \frac{1 - z^2}{1 + z^2} \quad z^2 = \frac{1 - t}{1 + t}.$$

After integration with the symmetry constraint  $\Theta(0) = 0$ , we obtain the solution

$$(A.8) \quad \left| \frac{(z - \sqrt{\mu})}{(z + \sqrt{\mu})} \right| = e^{2\beta x},$$

where

$$\beta = \sqrt{1 - \omega^2}, \quad \mu = \frac{1 - \omega}{1 + \omega}$$

and  $-1 < \omega < 1$ . Two separate cases are considered:

$$(A.9) \quad |z| \leq \sqrt{\mu} \quad z = -\sqrt{\mu} \frac{\sinh(\beta x)}{\cosh(\beta x)} \quad t = \frac{\cosh^2(\beta x) - \mu \sinh^2(\beta x)}{\cosh^2(\beta x) + \mu \sinh^2(\beta x)},$$

where  $t \geq \omega$ , and

$$(A.10) \quad |z| \geq \sqrt{\mu} \quad z = -\sqrt{\mu} \frac{\cosh(\beta x)}{\sinh(\beta x)} \quad t = \frac{\sinh^2(\beta x) - \mu \cosh^2(\beta x)}{\sinh^2(\beta x) + \mu \cosh^2(\beta x)},$$

where  $t \leq \omega$ . Let's introduce new parameters

$$\begin{aligned} A &= -2a_3 + a_4 + \frac{a_1 + a_2}{2}, \\ B &= -2a_4 + a_1 + a_2, \\ C &= 2a_3 + a_4 + \frac{a_1 + a_2}{2}. \end{aligned}$$

It is clear that  $A = \phi(-1)$  and  $C = \phi(1)$ . If  $t \geq \omega$  and  $\phi(t) \geq 0$ , it follows from (A.7) and (A.9) that

$$(A.11) \quad Q^+(x) = \frac{(1 - \omega)((\mu + 1) \cosh^2(\beta x) - \mu)}{(A\mu^2 + B\mu + C) \cosh^4(\beta x) - (B\mu + 2A\mu^2) \cosh^2(\beta x) + A\mu^2}.$$

If  $t \leq \omega$  and  $\phi(t) \leq 0$ , it follows from (A.7) and (A.10) that

$$(A.12) \quad Q^-(x) = \frac{(\omega - 1)((\mu + 1) \cosh^2(\beta x) - 1)}{(A\mu^2 + B\mu + C) \cosh^4(\beta x) - (B\mu + 2C) \cosh^2(\beta x) + C}.$$

The asymptotic behavior of the function  $Q(x)$  at infinity depends on the location of the zeros of the function  $\psi(\mu) = A\mu^2 + B\mu + C$ . The function  $\psi(\mu)$  is related to the function  $\phi(t)$ , e.g. if  $\psi(\mu) = 0$  then  $\phi(\omega) = 0$ .

**A.1. Case  $A < 0, C > 0$ .** In this case the quadratic polynomial  $\phi(t)$  has exactly one root  $\phi(t_1) = 0$  such that  $t_1 \in (-1, 1)$ . We have two branches of decaying solutions with the positive amplitude  $Q(x)$ . One branch occurs for  $t_1 < \omega \leq 1$  with  $Q(x) = Q^+(x)$  and the other one occurs for  $-1 \leq \omega < t_1$  with  $Q(x) = Q^-(x)$ . At the point  $\omega = t_1$ , the solution is bounded and decaying.

**A.2. Case  $A > 0, C > 0$ .** In this case the quadratic polynomial  $\phi(t)$  has no roots or has exactly two roots on  $(-1, 1)$ . If  $\phi(t)$  does not have any roots on  $(-1, 1)$ , we have a decaying solution with the positive amplitude  $Q(x)$  for any  $-1 < \omega < 1$  with  $Q(x) = Q^+(x)$ . If  $\phi(t)$  has two roots  $\phi(t_1) = 0$  and  $\phi(t_2) = 0$  such that  $t_1, t_2 \in (-1, 1)$  then we have a decaying solution with  $Q(x) = Q^+(x)$  only on the interval  $\max(t_1, t_2) < \omega \leq 1$ . At the point  $\omega = \max(t_1, t_2)$ , the solution becomes bounded but non-decaying if  $t_1 \neq t_2$  and unbounded if  $t_1 = t_2$ .

**A.3. Case  $A < 0, C < 0$ .** In this case the quadratic polynomial  $\phi(t)$  has no roots or has exactly two roots on  $(-1, 1)$ . If  $\phi(t)$  does not have any roots on  $(-1, 1)$ , we have a decaying solution with the positive amplitude  $Q(x)$  for any  $-1 < \omega < 1$  with  $Q(x) = Q^-(x)$ . If  $\phi(t)$  has two roots  $\phi(t_1) = 0$  and  $\phi(t_2) = 0$  such that  $t_1, t_2 \in (-1, 1)$  then we have a decaying solution with  $Q(x) = Q^-(x)$  only on the interval  $-1 \leq \omega < \min(t_1, t_2)$ . At the point  $\omega = \min(t_1, t_2)$ , the solution becomes bounded but non-decaying if  $t_1 \neq t_2$  and unbounded if  $t_1 = t_2$ .

**A.4. Case  $A > 0, C < 0$ .** In this case no decaying solutions with positive amplitude  $Q(x)$  exist.

**A.5. Special cases.** Two special cases occur when  $\phi(1) = 0$  or  $\phi(-1) = 0$ . If  $\phi(1) = 0$  then  $Q^+(x)$  has a singularity at  $x = 0$  for any  $-1 < \omega < 1$ . If  $\phi(-1) = 0$  then  $Q^-(x)$  has a singularity at  $x = 0$  for any  $-1 < \omega < 1$ .

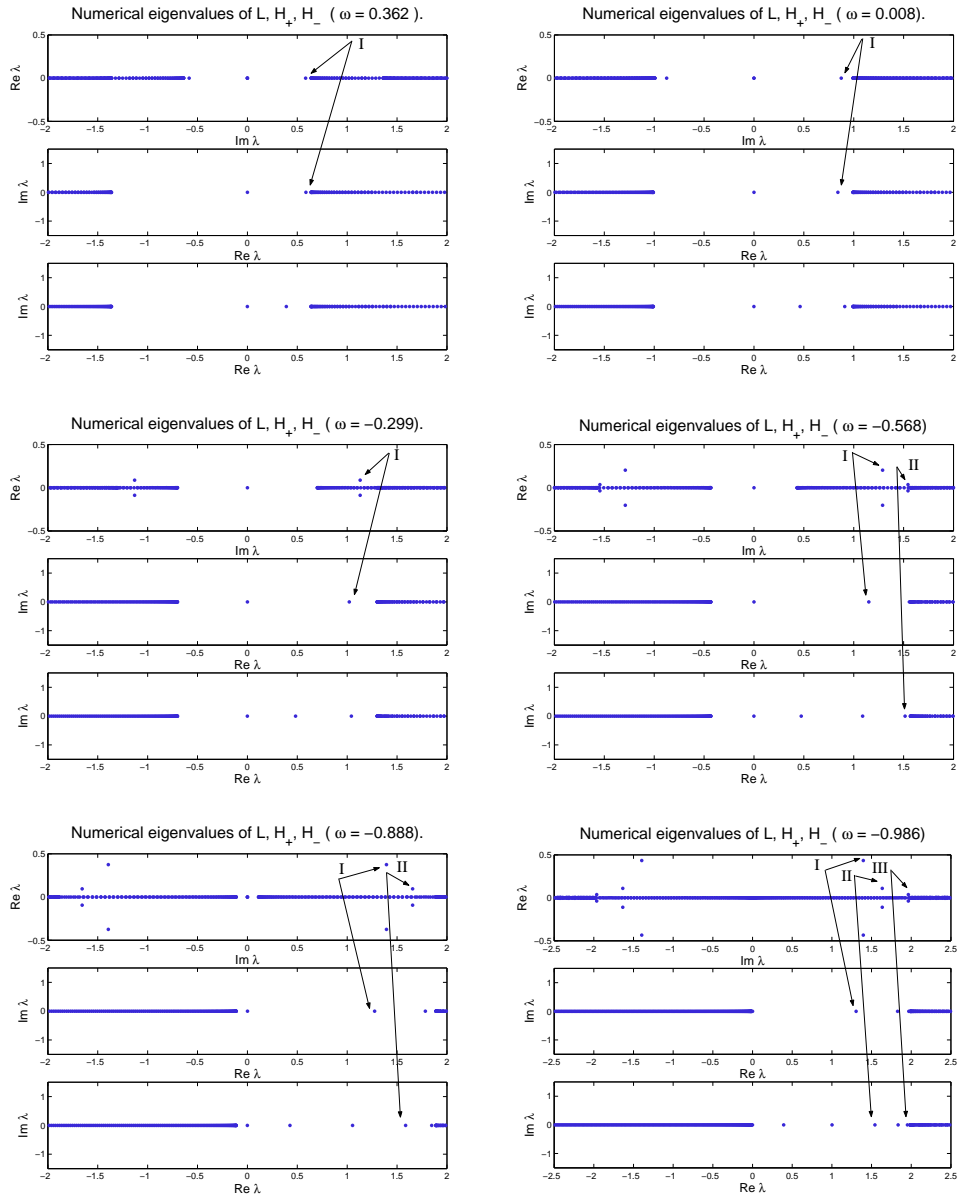


FIGURE 1. Eigenvalues and instability bifurcations for the symmetric quadric potential (2.5) with  $a_1 = 1$  and  $a_2 = a_3 = a_4 = 0$ .

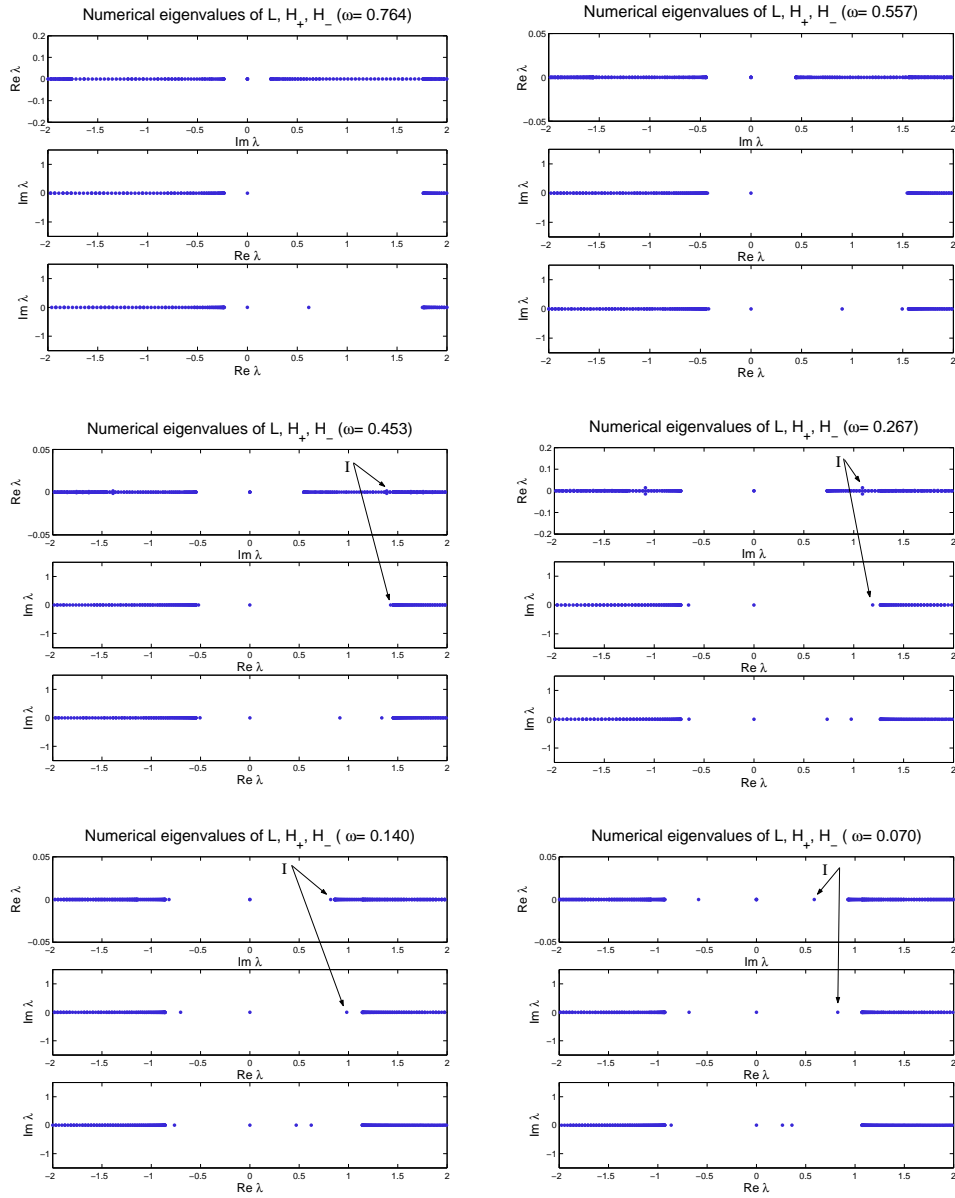


FIGURE 2. Eigenvalues and instability bifurcations for the symmetric quadric potential (2.5) with  $a_3 = 1$  and  $a_1 = a_2 = a_4 = 0$ .

## REFERENCES

1. C.M. de Sterke and J.E. Sipe, "Gap solitons", *Progress in Optics*, **33**, 203 (1994).
2. Yu. S. Kivshar and G.P. Agrawal, *Optical Solitons: From Fibers to Photonic Crystals* (Academic Press, San Diego, 2003).
3. E. Cornell and C. Wieman, "Bose–Einstein condensation in a dilute gas, the first 70 years and some recent experiments", *Rev. Mod. Phys.* **74**, 875–893 (2002)
4. C.M. de Sterke, D.G. Salinas, and J.E. Sipe, "Coupled-mode theory for light propagation through deep nonlinear gratings", *Phys. Rev. E* **54**, 1969–1989 (1996).
5. D. Agueev and D. Pelinovsky, "Modeling of wave resonances in low-contrast photonic crystals", *SIAM J. Appl. Math.* **65**, ... (2005)
6. D.E. Pelinovsky, A.A. Sukhorukov, and Yu. S. Kivshar, "Bifurcations and stability of gap solitons in periodic potentials", *Phys. Rev. E* **70** 036618 (2004)
7. I.V. Barashenkov, D.E. Pelinovsky, and E.V. Zemlyanaya, "Vibrations and oscillatory instabilities of gap solitons", *Phys. Rev. Lett.* **80**, 5117–5120 (1998)
8. I.V. Barashenkov and E.V. Zemlyanaya, "Oscillatory instabilities of gap solitons: a numerical study", *Comp. Phys. Comm.* **126**, 22–27 (2000)
9. D.J. Kaup and T.I. Lakoba, "The squared eigenfunctions of the massive Thirring model in laboratory coordinates", *J. Math. Phys.* **37**, 308–323 (1996)
10. D.J. Kaup and T.I. Lakoba, "Variational method: How it can generate false instabilities", *J. Math. Phys.* **37**, 3442–3462 (1996)
11. J. Schollmann, "On the stability of gap solitons", *Physica A* **288**, 218–224 (2000)
12. J. Schollmann and A. P. Mayer, "Stability analysis for extended models of gap solitary waves", *Phys. Rev. E* **61**, 5830–5838 (2000)
13. T. Kapitula and B. Sandstede, "Edge bifurcations for near integrable systems via Evans function techniques", *SIAM J. Math. Anal.* **33**, 1117–1143 (2002)
14. D.E. Pelinovsky and A. Scheel, "Spectral analysis of stationary light transmission in nonlinear photonic structures", *J. Nonlin. Science*, **13**, 347–396 (2003)
15. G. Derks and G.A. Gottwald, "A robust numerical method to study oscillatory instability of gap solitary waves", *SIAM J. Appl. Dyn. Syst.* **4**, 140–158 (2005)
16. G. Schneider and H. Uecker, "Existence and stability of modulating pulse solutions in Maxwell's equations describing nonlinear optics", *Z. Angew. Math. Phys.* **54**, 677–712 (2003).
17. D.J. Kaup and A.C. Newell, "On the Coleman correspondence and the solution of the Massive Thirring model", *Lett. Nuovo Cimento* **20**, 325–331 (1977).
18. D.E. Pelinovsky, "Inertia law for spectral stability of solitary waves in coupled nonlinear Schrodinger equations", *Proc. Roy. Soc. Lond. A* **461**, 783–812 (2005).
19. Y. Saad, "Numerical methods for large eigenvalue problems", Manchester University Press, 60–101 (1992)
20. G.H. Golub, H.A. Van der Vorst, "Eigenvalue computation in the 20th century", *J. of Comp. and Appl. Math.* **123**, 35–65 (2000)
21. Cluser Idra is a part of the SHARCnet network of parallel processors distributed between eight universities in Southern Ontario, including McMaster University.
22. Y. Saad "Chebyshev techniques for solving nonsymmetric eigenvalue problem", *Mathematics of Computation* **42**, 567–588 (1984)

DEPARTMENT OF MATHEMATICS, MCMASTER UNIVERSITY, HAMILTON, ONTARIO, L8S 4K1, CANADA

*E-mail address:* chugunom@math.mcmaster.ca; dmpeli@math.mcmaster.ca